AGU PUBLICATIONS

JGR

Journal of Geophysical Research: Solid Earth

RESEARCH ARTICLE
10.1002/2017JB014690

Special Section:
Slow Slip Phenomena and Plate Boundary Processes

Spatiotemporal Variations in Slow Earthquakes Along the Mexican Subduction Zone

J. Maury[1,2], S. Ide[1], V. M. Cruz-Atienza[3], and V. Kostoglodov[3]

[1]Earth and Planetary Science, University of Tokyo, Tokyo, Japan, [2]Now at BRGM, Orléans, France, [3]Instituto de Geofisica, Universidad Nacional Autonoma de Mexico, Mexico City, Mexico

Abstract Slow earthquakes in Mexico have been investigated independently in different areas. Here we review differences in tremor behavior and slow slip events along the entire subduction zone to improve our understanding of its segmentation. Some similarities are observed between the Guerrero and Oaxaca areas. By combining our improved tremor detection capabilities with previous results, we suggest that there is no gap in tremor between Guerrero and Oaxaca. However, some differences between Michoacan and Guerrero are seen (e.g., SSE magnitude, tremor zone width, and tremor rate), suggesting that these two areas behave differently. Tremor initiation shows clear tidal sensitivity along the entire subduction zone. Tremor in Guerrero is sensitive to small tidal normal stress as well as shear stress, suggesting that the subduction plane may include local variations in dip. Estimation of the energy rate shows similar values along the subduction zone interface. The scaled tremor energy estimates are similar to those calculated in Nankai and Cascadia, suggesting a common mechanism. Along-strike differences in slow deformation may be related to variations in the subduction interface that yield different geometrical and temperature profiles.

Key Points:
- Along-strike variations in slow earthquakes are observed in the Mexican subduction zone
- Tremor is sensitive not only to tidal shear stress but also to tidal normal stress
- Scaled tremor energy is similar to values reported for Japan and Cascadia

Supporting Information:
- Supporting Information S1

Correspondence to:
J. Maury,
J.Maury@brgm.fr

Citation:
Maury, J., Ide, S., Cruz-Atienza, V. M., & Kostoglodov, V. (2018). Spatiotemporal variations in slow earthquakes along the Mexican subduction zone. *Journal of Geophysical Research: Solid Earth*, *123*. https://doi.org/10.1002/2017JB014690

Received 13 JUL 2017
Accepted 13 JAN 2018
Accepted article online 19 JAN 2018

1. Introduction

Analysis of slow earthquakes (i.e., slow slip events (SSEs), tremor, low-frequency earthquakes (LFE), and very low frequency (VLF) earthquakes) improves our understanding of subduction zones. Some studies (Mazzotti & Adams, 2004; Obara & Kato, 2016; Roeloffs, 2006) suggest that these events are related to megathrust earthquakes and could therefore be used to better constrain the earthquake cycle. Numerical models (Ariyoshi et al., 2012; Matsuzawa et al., 2010) show that the frequency of occurrence of SSEs and the migration speed of VLF swarms should increase before a great earthquake. Moreover, Shelly (2009) found, by careful analysis of LFE catalogs, a probable increase in creep during the 3 months preceding the M_w6.0 Parkfield earthquake. This suggests the need for a thorough analysis of the spatiotemporal variations and recurrence times of slow earthquakes to better understand the earthquake cycle.

Obara and Kato (2016) suggested that slow earthquakes could be used as an analog for great earthquakes. Indeed, their magnitudes are similar (Kao et al., 2009; Radiguet et al., 2012), they present clear segmentation (Obara, 2010), and they are easy to observe because their recurrence times are much shorter than those of regular earthquakes. Therefore, to better understand the seismogenic process in subduction zones, we need to study the segmentation of both slow and regular earthquakes. Slow earthquakes have already been studied in detail in two regions (Japan and Cascadia), thanks to exceptional observational networks (e.g., Obara, 2010; Wech, 2010). The data from these regions provide us with two slightly different reference models for the seismic cycle.

On the Philippine Sea Plate, downdip of the seismogenic zone, episodic tremor and slip (ETS) occurs. Segmentation of this area can be determined from the spatial extent of ETS (Obara, 2010). Downdip of the edge, where megathrust events occur, long-term SSEs are observed. In the case of the Bungo channel, slow earthquakes extend updip, linking deep tremors and shallow VLF earthquakes, which may correspond to a barrier to high-speed rupture (Hirose et al., 2010). These observations can be explained by structural features in the subduction zone interface. Short-term SSEs at Boso and Nankai have different recurrence intervals, possibly due to differences between the thermal regimes of these regions (Obara, 2011). Moreover, the gaps (Ise Bay, Kii Channel, and central Shikoku) in the segmentation of ETS seem to be related to topographic

features of the subducting plate (Obara, 2010). These also seem to be the case for shallow VLF events that occur in an area of low slip deficit rate, probably related to subducting seamounts (Yokota et al., 2016).

Seismic behavior in Cascadia is different to that in the Japan region. Seismicity is sparse but large earthquakes are known to occur (Mazzotti & Adams, 2004). In terms of slow earthquakes, only ETS occurs (Gomberg & The Cascadia 2007 and Beyond Working Group, 2010), and no long-term SSEs have been detected. SSEs behavior is very uniform, with similar slow events along the entire 1,000 km of the subduction zone. Subduction zone is segmented in broad areas where ETS have distinct recurrence intervals, and their spatial extent corresponds to changes in geological terranes (Brudzinski & Allen, 2007). This segmentation can also be related to topography of the subduction interface. These findings suggest that slow event segmentation is linked to the large-scale properties of the plate interface. In general, analysis of similar observations at another subduction zone could improve our understanding of the state of stress and the possible causes of barriers to slip.

Here we focus on the Mexican subduction zone. We know that tremor and SSEs occur in different segments of the plate interface (Kostoglodov et al., 2010); however, we lack a broader perspective on the overall behavior of these phenomena along the coast, which could allow us to identify similarities or differences between segments. This could eventually help us to determine whether the subduction system is similar to those at Cascadia or Japan. To date, tremors in Mexico have been studied only in isolated places (e.g., Brudzinski et al., 2010, 2016; Husker et al., 2012) rather than as a continuous phenomena. Even if tremor is mainly detected using temporary networks, some comparisons are still possible. Thus, the aim of this study is to obtain a general overview of slow earthquakes in the Mexican subduction zone.

Tremors in northwest Mexico are sparse and occur in isolated clusters (Ide, 2012), while tremors in Guerrero are more frequent and are separated into two clusters along dip (e.g., Cruz-Atienza et al., 2015; Frank et al., 2014; Maury et al., 2016; Payero et al., 2008). The updip tremors in Guerrero (the transient zone) occur mainly during long-term SSEs (Husker et al., 2012; Kostoglodov et al., 2010), but the downdip cluster, often called the "sweet spot", is active more continuously. Tremors in the southeast (i.e., in Oaxaca) are frequent but not significantly modulated by long-term SSEs (Brudzinski et al., 2010). Overall, tremor occurs in places where no other seismicity is recorded (Figure S1 in the supporting information). In this study we consider the similarities and differences between different segments of the Mexican subduction zone in more detail.

In the Mexican subduction zone, the remains of the Farallon plate, the Cocos, and Rivera plates subduct in approximately NE direction under the North America plate (Figure 1). The Cocos and Rivera plates are relatively young, less than 20 Ma at the trench. The subduction velocity in the area of interest, between Oaxaca and Jalisco states (Figure 1), varies between 7.0 and 5.5 cm/yr from SE to NW (DeMets et al., 2010). The subduction interface geometry is segmented along the coast with one dominant feature between −101° and −96° where it is subhorizontal at 40 km depth for about 200 km downdip.

To perform our analysis, we review SSEs along the subduction zone interface and examine the tremor and VLF events behavior to determine spatial variations along strike in the subduction zone. Seismic analysis principally uses data recorded by temporary networks, so our observations are spatially and temporally limited, and we must therefore make inferences about the studied areas. Finally, we relate these observations to the structure of the oceanic slab.

2. Slow Slip Events

Long-term SSEs are observed in two main areas along the Mexican subduction zone, in Guerrero (Franco et al., 2005; Iglesias et al., 2004; Kostoglodov et al., 2003; Larson et al., 2007; Lowry et al., 2001; Radiguet et al., 2012) and in Oaxaca (Brudzinski et al., 2007; Graham et al., 2014, 2016). In Guerrero, probably the largest events in the world occur downdip of the Guerrero seismic gap. These events are limited to longitudes between −101.5° and −99° (Figure 1) and have magnitudes of ∼7.5. They nucleate in the subhorizontal part of the subduction interface (approximately at 40 km depth) and propagate updip, partly into in the seismogenic part of the zone (e.g., Radiguet et al., 2016). These events occur every 4 years and last nearly a year (Figure 2). In addition, Frank et al. (2015) used summations of GPS time series aligned at the moments of LFE bursts and detected short-term SSEs downdip of the slip area of the larger long-term events, which have been recently shown to take place in the sweet spot (Villafuerte & Cruz-Atienza, 2017). These short-term SSEs have a maximum magnitude of 6.4 and a recurrence period of about 90 days.

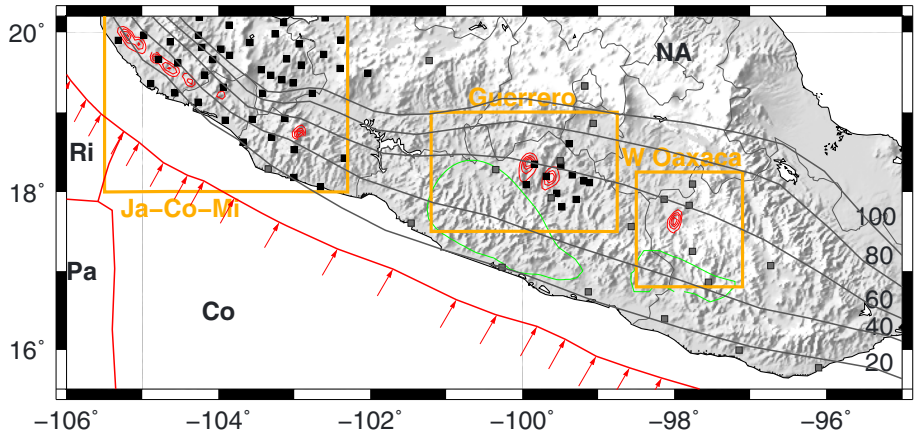

Figure 1. Seismic overview of the Mexican subduction zone. The three areas studied are indicated by orange rectangles. Red contours correspond to tremor density. Green contours are slip contours for the 2009–2010 Guerrero SSE (Radiguet et al., 2012) and the 2008–2009 Oaxaca SSE (Graham et al., 2016). Squares indicate seismic stations used (black = temporary stations; gray = permanent stations). Red lines indicate plates boundaries and red arrows convergence rates (DeMets et al., 2010). The gray lines here and in the following figures are the subducting slab contours from Pardo and Suárez (1995). Co = Cocos Plate; Ri = Rivera Plate; NA = North America Plate; Pa = Pacific Plate.

The long-term SSEs in Oaxaca are smaller than in Guerrero (Figures 1 and 2), ~M_w7.0, repeating every 1–2 years, and last only 6 months. They are limited to the downdip part of the seismogenic zone and are located along strike between −96° and −98°, with some events extending to −99° (e.g., the M_w7.2 2010–2011 event). These two types of SSEs, in Guerrero and Oaxaca, have nucleation zones separated by about 300 km, but some events propagate into this area (Graham et al., 2016).

Farther west, in the Jalisco-Colima-Michoacan (Ja-Co-Mi) area, SSEs have only been recently reported (Brudzinski et al., 2016) and they are not as well constrained. The GPS displacements observed are close to the noise level, which suggest that these events are much smaller than SSEs in Guerrero. These small SSEs are located at the Cocos-North America interface; farther west some even smaller events could exist at the Rivera-North America subduction interface. Between these small events and Guerrero SSEs is a gap (~ −101.5° to −103.5°) where no SSE has been observed. This gap could be an artifact due to the lack of local GPS stations, but considering the very different SSEs magnitudes on either side of the gap, it could be real.

Based on all SSEs observations we can already distinguish the Ja-Co-Mi area, where only small short-term SSEs occur, from Guerrero and Oaxaca where long-term SSEs also occur regularly. Considering the location of the SSEs (spatial extension into the seismogenic zone in Guerrero and not in Oaxaca), their relative sizes (M_w7.5 versus 7.0) and their recurrence intervals (4 years versus 1–2 years), we can further distinguish between Guerrero and Oaxaca (Figure 2), but these are less prominent differences.

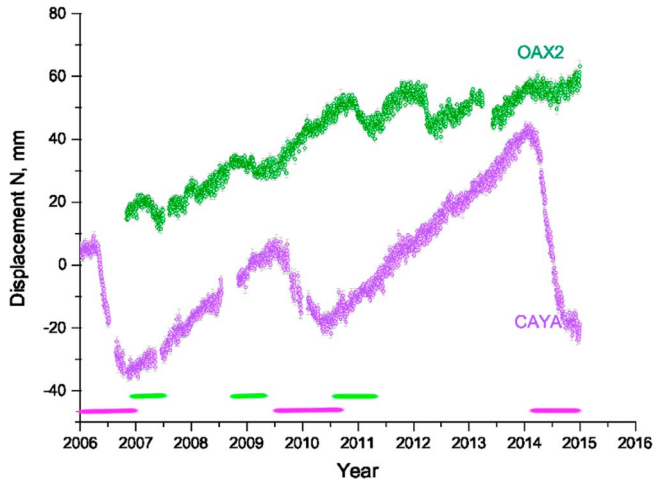

Figure 2. Time series for the north component of two stations in Guerrero (CAYA) and Oaxaca (OAX2). The pink and green bottom lines indicate SSEs for Guerrero (Radiguet et al., 2012, 2016) and Oaxaca (Graham et al., 2016), respectively.

3. Tremor Detection and Location

3.1. Seismic Data

We focus on three areas for which data are available from either a temporary network or a sufficient number of permanent stations from the National Seismological Service (SSN) network: Ja-Co-Mi, Guerrero, and Western Oaxaca (Figure 1).

For the Ja-Co-Mi area we mainly use temporary stations from the Mapping the Rivera Subduction Zone (MARS) experiment (Yang et al., 2009). These were broadband stations with a relatively dense array distribution in this area (Figure 1); the mean interstation distance was 70 km. These stations were installed for 1.5 years beginning in January 2006. Additionally, one permanent station (MMIG) is available during the time that the MARS stations were in service.

Table 1
Tremor Area Width and Mean Depth in Several Subduction Zones

Zone	Width (km)	Depth (km)	Source[a]
Ja-Co-Mi	20	25 to 38	This study
Guerrero G-GAP	39[c] and 87[b]	39	This study
Guerrero MASE	26[c] and 74[b]	38	Maury et al. (2016)
W Oaxaca	45	34	This study
Nankai	23	34	Idehara et al. (2014)
Cascadia	55 to 25	30	Idehara et al. (2014)
S Chile	19	38	Idehara et al. (2014)

Note. For details of the calculation method, see text.
[a]Width and depth estimated from tremor catalogs cited. [b]Width including the transient zone and sweet spot. [c]Width including only the sweet spot.

In Guerrero, two temporary networks were deployed at different times (Maury et al., 2016). However, since we focus on along-strike variations in slow earthquakes, we only use data from the G-GAP temporary network, which is better suited to this purpose. This network comprises mainly vertical short-period sensors with four 40 s three-component sensors (Zigone et al., 2012). In addition we use data from seven permanent SSN stations (http://www.ssn.unam.mx). These stations are located around the main tremor cluster and the interstation distance is about 40 km. We study a 3 year period in Guerrero beginning at the end of 2010 with a 6 months gap in 2012 due to the absence of enough data from the G-GAP network.

For Western Oaxaca, we use only permanent SSN stations. We begin our analysis at the end of 2012, when we have enough stations ($\geq$10) to adequately detect tremors. The interstation distance is 80 km. We analyze data through the middle of 2015, which gives a study window of 2.5 years.

The Guerrero network is the most appropriate to detect tremors, and the SSN network in Oaxaca has limited coverage in a narrow area.

3.2. Spatiotemporal Variations in Tremor

To locate tremor we use a method based on cross correlation of the seismic envelope which has been used previously in several regions (e.g., Ide, 2012; Idehara et al., 2014; Maury et al., 2016). We use 300 s windows with a lag of 150 s and band-pass filter data between 2 and 8 Hz. We utilize horizontal component data from all stations except the G-GAP temporary network, for which only vertical-component data are available. Since we have a limited number of stations in Oaxaca and Ja-Co-Mi, we declare tremor detection when a correlation threshold of 0.5 is exceeded for at least five pairs of stations. Considering this relatively low detection threshold, in a second step, we use a clustering technique to limit false detections (Ide, 2012). We only retain events that are within a 1 h window and 10 km distance to one other event.

Figure 3 shows that the spatiotemporal patterns of tremor in Guerrero and Western Oaxaca are similar (e.g., similar location along dip), suggesting continuity between the two zones. While no tremor has been detected in the gap between these two areas, this is probably due to a lack of station coverage rather than a lack of tremor. On the other hand, there is a clear change in tremor occurrence between Guerrero and Ja-Co-Mi. In Guerrero and Oaxaca, tremors occur at about 40 km depth in an area that is 40–50 km wide. In Ja-Co-Mi, tremor depth varies from 40 km in the eastern part of the zone to 25 km in the west. We can estimate the tremor area width by taking bins of 10 km width with a lag of 5 km along strike. Then, we define the tremor width of this bin as the area containing 90% of the tremors, provided that more than 20 tremors are located in the bin. The width of this area is defined as the mean value of all bins, but if the tremor width is varying (i.e., a histogram presents two peaks; see supporting information Figure S2), two values are used. The tremor width in Ja-Co-Mi is only 20 km but almost 80 km in Guerrero and 45 km in Oaxaca. If we compare the present data with other areas worldwide that produce tremors (Table 1), the tremor width is relatively small in Ja-Co-Mi, relatively large in Guerrero, and progressively narrows as we approach Eastern Oaxaca (Fasola et al., 2016). In fact, tremor area width in Guerrero is largest if we consider the transient zone. Tremor widths in Guerrero and Oaxaca are similar to those in northern Cascadia, while the tremor width in Ja-Co-Mi is similar to that of Nankai. On the other hand, tremor depth (Table 1) is relatively similar worldwide (between 30 and 40 km). The only exception is tremor in Jalisco that is shallower (mean value of 25 km) than in every other subduction zone.

The temporal variations (Figure 3) show that Ja-Co-Mi tremors occur sparsely in space and time, and there is no clearly defined long-lasting tremor patch, while tremor clusters in Guerrero and Oaxaca can extend to the whole zone along strike (~100 km). In Guerrero, tremors occur nearly continuously at a high rate (Figure 4). In Western Oaxaca, tremors are also nearly continuous but with a gap in January 2014, which is unexplained. In Ja-Co-Mi, the tremor activity is much lower and the tremor rate rarely exceeds 10 tremors/d (Figure 4) compared with Oaxaca (which is covered by a sparse network and therefore less sensitive detection).

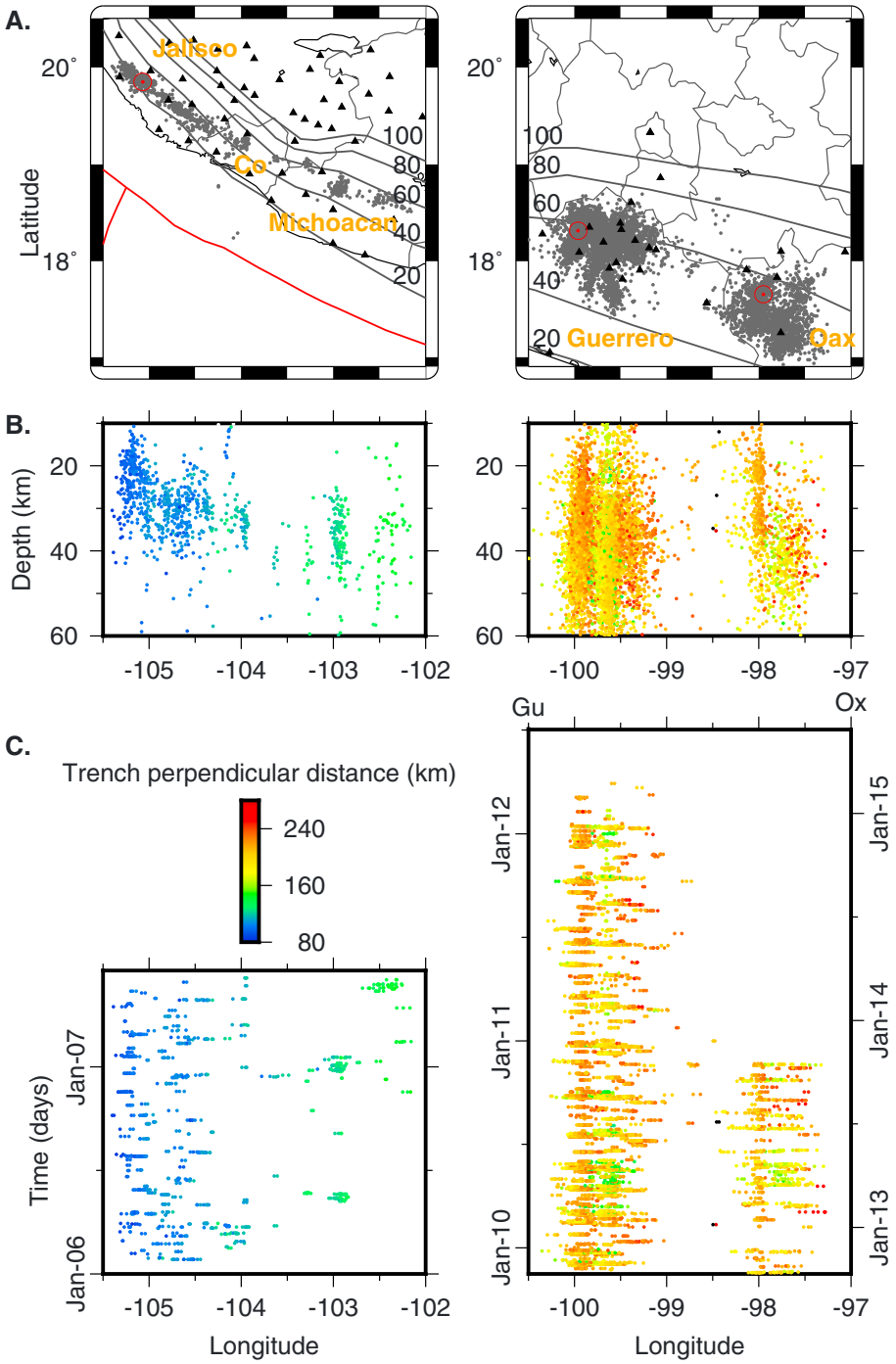

Figure 3. Spatiotemporal variations in tremors. (a) Tremor locations in the three areas studied. Red circles indicate areas used for tremor counts in Figure 4. Co = Colima; Oax = Oaxaca. Triangles indicate seismic stations used. (b) Tremor depth as a function of longitude (approximately along-strike evolution). (c) Tremor evolution in time as a function of longitude. Colors correspond to trench perpendicular distances.

4. Tremor Tidal Sensitivity

Tremor has been shown to be sensitive to tides in several regions (Houston, 2015; Nakata et al., 2008; Thomas et al., 2009). In Mexico, only Ja-Co-Mi tremors have been studied (Ide, 2012), suggesting a strong tidal sensitivity. Peng and Rubin (2017) studied tremors in Guerrero and found their periodicity close to 12.4 h that could be related to tidal forcing. However, if we look at the tremor duration, we can observe that tremors in Ja-Co-Mi

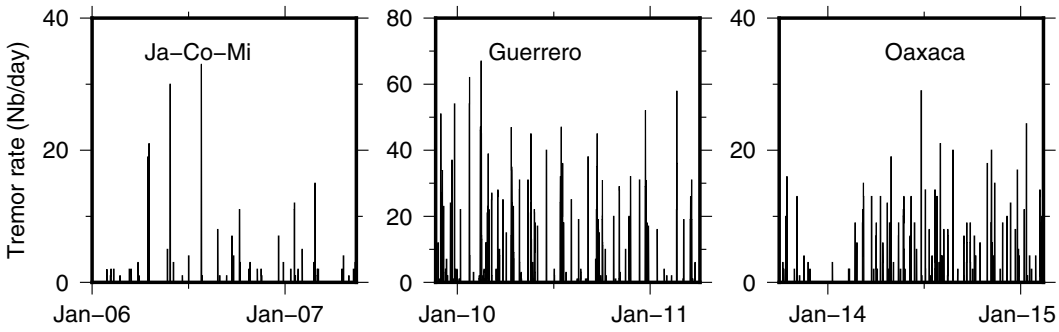

Figure 4. Hourly count of tremor (number per day) for each region during a 500 days window. An area of 20 km radius is used to build each histogram (see Figure 3).

are of short duration, around 20 s, while those in Guerrero are of longer duration (50–100 s). The tremor duration is related to tidal sensitivity (Ide, 2012), with short-duration tremors more likely to be sensitive to tides. Here we quantify the tremor tidal sensitivity in all regions of Mexico.

To estimate tidal sensitivity, we follow Yabe et al. (2015). We assume that the relationship between tremor rate and tidal stress is exponential:

$$R(\sigma) = R_0 \exp(\alpha\sigma), \tag{1}$$

where R_0 is a reference tremor rate, σ is either the tidal shear stress or tidal normal stress, and α (kPa^{-1}) is the tidal sensitivity. If $\alpha = 0$, tremors are not sensitive to tides, but if $\alpha \gg 0$, tremors are sensitive. A negative value means that tremors are more likely to occur when tidal stresses resist failure, which, in most cases, does not have a physical meaning. The parameter σ is calculated from the tidal stress tensor, estimated using both body and ocean tides. Sea level change is calculated using the SPOTL program (Agnew, 2012). The stress tensor is estimated every 0.1° in latitude and longitude at the tremor depth: 40 km for Guerrero and Oaxaca, and the mean tremor depth in a 20 km radius of each point is considered for Ja-Co-Mi. The stress tensor is then converted to traction on the fault using the subduction strike, dip, and rake estimated from analysis of VLF events, in section 6, in Guerrero and Oaxaca (strike of 292°, dip of 6°, and rake of 87°). For Ja-Co-Mi, we take values consistent with our analysis but not precisely equal to these values: we use a strike of 300° for the Michoacan area and 310° for the Jalisco area, a dip of 40°, and rake for a pure thrust event. The α is estimated using the maximum likelihood method for grid points having more than 100 tremors in a 20 km radius. The maximum likelihood becomes maximum when its derivative is zero; that is,

$$\frac{\int_{\sigma_{\min}}^{\sigma_{\max}} \sigma B(\sigma) \exp(\alpha\sigma) \mathrm{d}\sigma}{\int_{\sigma_{\min}}^{\sigma_{\max}} B(\sigma) \exp(\alpha\sigma) \mathrm{d}\sigma} - \frac{\sum_{i=1}^{N} \sigma_i}{N} = 0, \tag{2}$$

where the summation is over the ith tremor that occurred at stress level σ_i, N is the number of tremors, and $B(\sigma)$ is the time distribution density function. For details on the calculation of the likelihood, the reader is referred to Yabe et al. (2015).

Figure 5 shows the calculated tidal sensitivities in the Mexican subduction zone. As observed by Ide (2012), tremors in Ja-Co-Mi are highly sensitive to tidal shear stress, but there are some variations; for example, the southeastern events are not very sensitive to tides (Figure 5c and Figure S2 in the supporting information). Tremors in Guerrero and Western Oaxaca are largely insensitive to, or negatively correlated with, tidal shear stress, but they are sensitive to normal stress. The opposite relationship is seen in most onshore regions, where tidal shear and normal stresses are generally anticorrelated (Figures 1e–1f, Yabe et al., 2015). Because of the subhorizontal orientation of the subduction plane, tidal stresses are very low in Guerrero and Oaxaca, nearly 1 order of magnitude smaller than in Jalisco (Figure 5a), and the normal stress is even smaller than the shear stress; this also explains why the uncertainty of α is higher in these regions (Figure 5d and Figure S5 in the supporting information). However, considering the high value of α for normal stresses in Guerrero (~2 in some places), even with such a high uncertainty (at most ±0.6 kPa^{-1}), the results seem reliable.

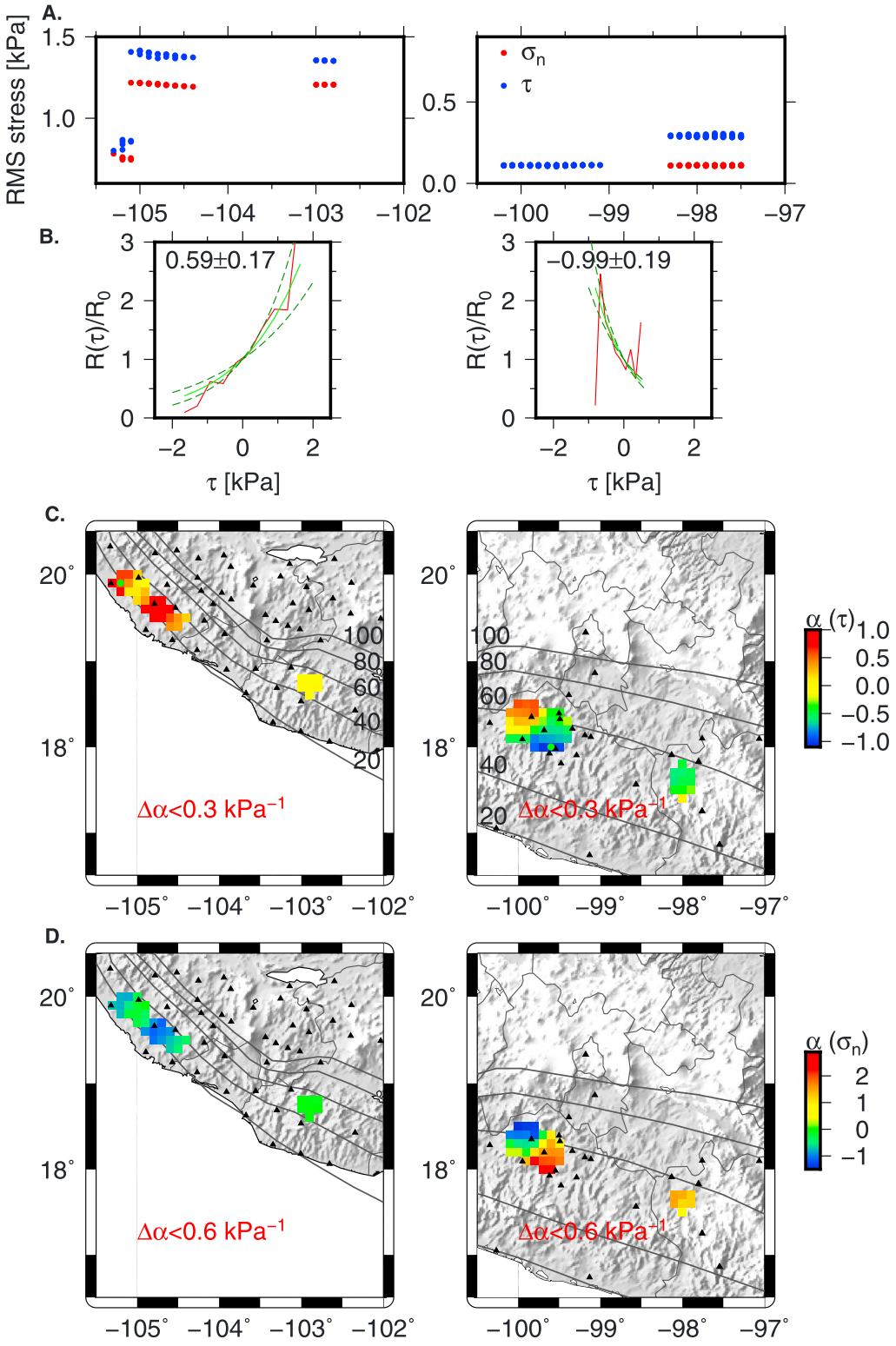

Figure 5. Tidal sensitivity. (a) RMS values of shear stress τ and normal stress σ_n as functions of longitude at points where >100 tremors are available. (b) Tremor sensitivity to tidal shear stress. Comparison between observed (red line) and calculated (green line) normalized tremor rates for two points. The dotted lines show the uncertainties. (c) Spatial distribution of tidal sensitivity α to shear stress. Only tidal sensitivity values with errors $\Delta\alpha < 0.3$ kPa^{-1} are considered. The green dots indicate the points shown in Figure 5b. (d) Spatial distribution of tidal sensitivity α to normal stress. Tidal sensitivity values with $\Delta\alpha < 0.6$ kPa^{-1} are considered because of higher uncertainty in Guerrero and Oaxaca. All points in Ja-Co-Mi have $\Delta\alpha < 0.3$ kPa^{-1}.

Moreover, the correlation between observed and calculated tremor rates is very high (Figure 5b and Figure S4 in the supporting information), even over a short stress range.

We may therefore conclude that tremors in Jalisco are highly sensitive to tidal shear stress, while tremors in Guerrero and Oaxaca seem more sensitive to tidal normal stress.

5. Seismic Energy of Tremors

To better characterize tremor behavior, we focus on its energy. Following Yabe and Ide (2014) the energy for event *i* at station *j* is determined by

$$E_{ij} = 4\pi R_{ij}^2 \rho\beta \int \dot{u}_{ij}^2(t)\mathrm{d}t \times \exp(2CR_{ij}) \times \frac{1}{S_j^2}, \tag{3}$$

where E_{ij} is the source energy term; ρ and β are the density and *S* wave velocity in the focal region, respectively; $\dot{u}_{ij}$ is the ground velocity at the station in the frequency range 2–8 Hz; R_{ij} is the hypocentral distance; and S_j is the station amplification factor. $C = \frac{\pi f}{Q\beta}$ represents the path attenuation where *f* is frequency and *Q* the quality factor. We use frequencies between 2 and 8 Hz, because the tremor signal is dominant in this frequency band (Yabe & Ide, 2014).

We assume values of $\rho = 2{,}700$ kg/m^3, $\beta = 3{,}500$ m/s, and $C = 3 \cdot 10^{-6}$ m^{-1} following Yabe and Ide (2014), who studied the Ja-Co-Mi area.

The energy for tremor *i* detected at *N* stations is then treated as the mean value of the logarithm:

$$\log(E_i) = \frac{1}{N}\sum_{j=1}^{N} \log(E_{ij}). \tag{4}$$

Because our tremor catalog is incomplete (we detected at most one event in each 300 s window), we use an energy rate that does not depend on catalog completeness. We divide the energy by the tremor duration, defined as the half width of the stacked envelope.

To determine site amplification factors, we use the coda normalization method for regional events (e.g., Kato et al., 1995) in the tremor frequency band of 2–8 Hz. This method assumes that at times longer than twice the *S* wave travel time, the signal consists of scattered waves and does not depend on distance or the source radiation pattern. The amplification factor is then determined by the ratio

$$\frac{A_{ij}(f,t)}{A_{ik}(f,t)} = \frac{W_i(f)G(f,t)S_j}{W_i(f)G(f,t)S_k} = \frac{S_j}{S_k}, \tag{5}$$

in which $A_{ij}(f,t)$ is the spectral amplitude of the coda wave for the *i*th event at the *j*th station, W_i is the source term, and $G(f,t)$ is the path term. We use seven time windows of 10 s with lags of 5 s for each event. If the average amplitude of a signal window is lower than twice the average amplitude of the noise in a 10 s window beginning 30 s before the earthquake, we discard it. We then solve a linear inverse problem for the logarithmic site amplification factors:

$$\log(A_{ij}(f,t)) - \log(A_{ik}(f,t)) = \log(S_j) - \log(S_k) + e_{ijk}, \tag{6}$$

in which we assume that the error e_{ijk} has a standard normal distribution. An additional constraint is required to solve the problem uniquely, so we fix $S_1 = 2$ for the reference station. We use TLIG as the reference station because it is a permanent SSN station, and we set this factor to 2 to account for the free surface effect. All site amplification factors along the subduction zone are determined relative to this station. For these calculations, we determined factors for several zones, from Jalisco to Oaxaca, with at least two common stations in each zone. Only events within 150 km of a station and between 10 and 50 km depth were used. In total, we used about 2,000 events for Oaxaca, 1,000 for Guerrero, 100 for Michoacan, and 30 for Jalisco-Colima. The differences in sample sizes are due to regional differences in seismicity rates and variations in the operational window lengths of the different temporary networks.

Figure S6 (supporting information) shows the site amplification factor, and Figure 6 shows the energy rate variations. We can observe good general agreement in energy rate values between the different zones. The energy rate presents along-strike variations between Jalisco and Michoacan, with higher values in Jalisco.

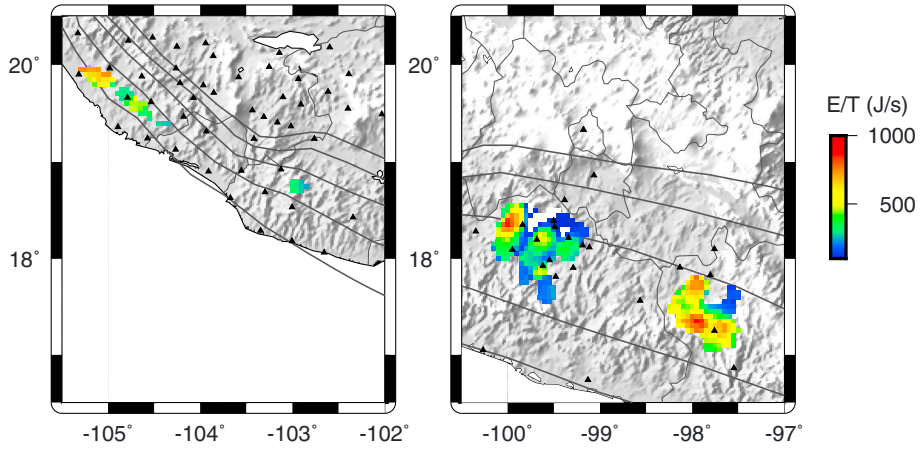

Figure 6. Spatial distribution of tremor energy rates defined as the median of the size-frequency statistic (Yabe & Ide, 2014). A grid of 0.05° is defined, and the energy rate is calculated for points with more than 50 tremors within a 10 km radius.

Slightly higher energy rate values are observed in Guerrero and Oaxaca than in Ja-Co-Mi. Higher values are detected updip in Western Oaxaca, as was observed in Nankai and Western Shikoku (Yabe & Ide, 2014). We do not see such features anywhere else, because the tremor width is too small in Ja-Co-Mi and because updip tremors in Guerrero (the transient zone) are less energetic and not well detected (Husker et al., 2012).

6. VLF Event Analysis

VLF events often occur simultaneously with tremors. To detect them, and to determine the focal mechanism of these slow events, we stack waveforms in the VLF band (0.02–0.05 Hz). We apply the same stacking method as used in many other regions (Ide, 2016; Ide & Yabe, 2014; Ide et al., 2015; Maury et al., 2016). We use a grid with 0.1° increments in latitude and longitude. If more than 100 tremors are within a 10 km radius of a grid point, we stack the waveforms. Because few tremors are detected in Ja-Co-Mi, we only stack events at the locations of the four main clusters and use a radius of 12 km to encompass the entire cluster. Even with this

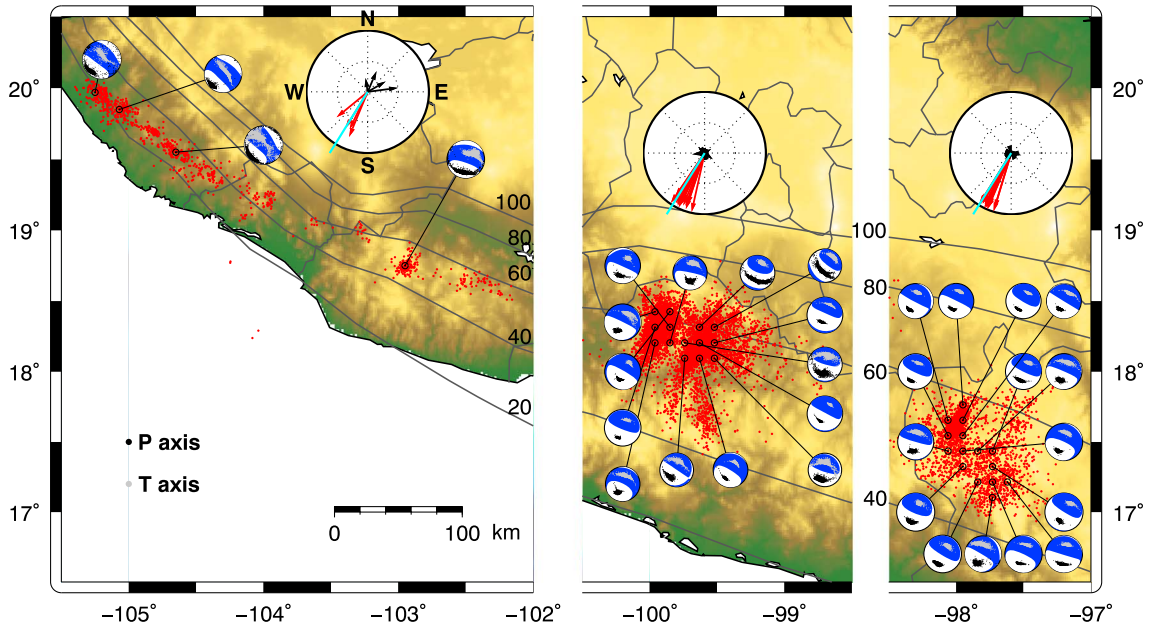

Figure 7. Focal mechanisms of VLF events. Black and gray dots indicate *P* and *T* axis from 2,000 bootstrap resampling tests, respectively. Red points show tremor locations. Grid points are indicated by open circles. The inset shows the direction of the fault-normal (black) and slip (red) vectors. Light blue lines in figure insets indicate the direction of plate convergence.

extended criteria, we have few tremors to stack (140 at maximum), so the resulting moment tensors are less well resolved than in other areas. For this analysis, in Guerrero, we can only use the permanent stations and not the temporary stations of the G-GAP network because they are short-period instruments. However, the stations in Oaxaca are appropriate for stacking because they are broadband and cover a large azimuthal range, and VLF events are detected farther away than tremors. Thus, the Oaxaca area should provide reliable results. Because of these constraints in station coverage and number of tremors available to stack, we neglect the isotropic component of the moment tensor.

The VLF focal mechanisms (Figure 7 and Table S1 in the supporting information) indicate shear thrusting with a nearly horizontal fault plane in Guerrero and Western Oaxaca. The similarity between mechanisms in Guerrero and Oaxaca is striking and indicates that the subduction plane is still subhorizontal in Western Oaxaca, as suggested by Pardo and Suárez (1995). The slip directions agree with the direction of plate convergence (compare with the stereographic slip projections) estimated by DeMets et al. (2010). For the Ja-Co-Mi area, the fault plane in Michoacan is less inclined than expected and the mechanisms less well resolved everywhere, as expected, but results are still similar to those obtained to the SE and are consistent with our knowledge of the plate interface geometry. The dip of about 40° for the Rivera Plate in Ja-Co-Mi differs significantly from that observed in Guerrero and Oaxaca but is in accordance with that suggested by Pardo and Suárez (1995).

7. Discussion

7.1. Error Assessment

We applied several methods to better characterize slow earthquakes, in order to develop a broader perspective of their behavior along the entire Mexican subduction zone. However, we must consider the uncertainty of each method before drawing robust conclusions.

For tremor location, an error estimation is difficult. Ide (2010b) compared regular earthquakes locations in Nankai determined by envelope cross correlation with locations obtained by the Japan Meteorological Agency (JMA). The distribution of the differences between locations has a mean close to 0 km, and a standard deviation of about 1 km in the horizontal and 5 km in the vertical. Station coverage in Mexico is not as dense as in Japan but remains acceptable for our purposes. We attempted the same analysis in Mexico as in Japan; however, the number of earthquakes from the ISC catalog (Storchak et al., 2013; and Figure S1) is limited: the catalog comprises 10 events in Ja-Co-Mi, 114 in Guerrero, and 20 in Oaxaca, so the results yield only qualitative tendencies and statistical significance cannot be assessed. The distributions of the differences between horizontal locations in Guerrero, Oaxaca, and Ja-Co-Mi have mean values of 8, 11, and 29 km, respectively, with standard deviations of 6, 18, and 21 km, respectively. The differences in vertical locations globally exceed those in horizontal locations, which is expected, with mean differences of 11, 14, and 20 km. These differences in precision are due partly to the paucity of recorded earthquakes in Ja-Co-Mi and Oaxaca compared with Guerrero. However, these variations are also due to differences in network distribution, with the Guerrero stations being more suitably oriented. The lowest precision is obtained in Ja-Co-Mi, but this is also the area where tremors are the most clustered, giving more weight to their relative locations. We apply a clustering technique to limit false detections, and our locations are in agreement with previous results in each zone (Ide, 2012; Fasola et al., 2016; Maury et al., 2016) using different stations and methods for Guerrero and Oaxaca. Using earthquake locations, we can estimate a precision of 20 km for tremor locations. For these reasons, we believe that each tremor patch we detected is distinct.

The uncertainty in tidal sensitivity of tremor has been quantified by Yabe et al. (2015). They found that even if tremor selection is not made by statistical analysis (i.e., with some inherent error that cannot be quantified by the maximum log likelihood method), their results coincide with those based on a frequency method (e.g., Ide, 2012). Thus, the results are robust with respect to that technique. In this study, we only retain α values with error lower than 0.3 kPa^{-1} in order to draw comparisons using only the most reliable results (Figure S5). However, due to the low normal stress in Guerrero and Oaxaca, the calculation is made over a very short stress range, and is less well constrained (maximum error of 0.6 kPa^{-1}) than in other areas (Figure S3). Despite this limitation, we obtain an α value so high (close to 2) that we can be relatively certain of our results in these provinces.

The error in the energy is estimated from the standard deviation of the mean $\log(E_i)$. This error is mostly within a factor of 2 of the energy estimated (Figure S5) except in Colima and Michoacan, where the stations are

at varying distances from the tremor sources and the factor is around 3. However, there is also an intrinsic error that depends on the parameters used for the energy calculation, including the tremor centroid locations. The energy calculation is strongly dependent on the station corrections; these are well determined in Guerrero and Oaxaca whereas the small number of earthquakes in Jalisco and Michoacan (Figure 1) means that we have fewer amplitude ratio values in this area. However, the number of stations is higher in this area, counterbalancing this somewhat. One remaining uncertainty in our stations parameters in Ja-Co-Mi is their values relative to station TLIG in Oaxaca. However, we used permanent stations for this link; thus, even though there are relatively few (ARIG, MMIG, MOIG, and ZIIG), we have about 10 years of data from each station, adding many more events than those detectable during the relatively short lifespan of the MARS network. We can therefore conclude that these station correction factors are robust. Another uncertainty is the effect of attenuation; we use a value of attenuation estimated for the Ja-Co-Mi area everywhere, which may not be accurate. Several attenuation studies have surveyed the region (e.g., García et al., 2005; Yabe & Ide, 2014), and the resultant values vary. However, if we consider a mean hypocentral distance of 70 km, changing the rock-quality factor Q from 500 to 1,000 changes the energy by less than a factor 2, so this choice of attenuation is not expected to have a noticeable impact on our results. As noted previously there is some uncertainty in tremor locations. The effect of centroid location uncertainty on energy will be limited, because we use the mean energy estimated at every station. Because of each network's azimuthal coverage, the tremor centroid location too far from one station will be closer to another. Furthermore, a 10 km variation in location at a mean distance of 70 km changes the energy estimate by less than a factor of 2. We can therefore conclude that our energy estimates are robust considering the location uncertainties.

Considering the moment tensor, we can obtain a reliable estimate of the uncertainty by bootstrap resampling. In Guerrero and Oaxaca, the moment tensors appear to be well constrained: the dips of the P and T axes vary by <5° and the strikes lie within 15° for Oaxaca and 20° for Guerrero. However, some caution must be taken when interpreting solutions obtained in Ja-Co-Mi: the dips of P and T axes lie within 5° and within 10°, respectively, but the strikes have respective ranges of 20° and 40° (Table S1). Nonetheless, considering that these solutions are consistent with previous solutions and consistent with the geometry of the plate interface, we can be confident that they are sufficiently accurate.

7.2. Slow Earthquakes Characteristics Along the Mexican Subduction Zone

Analyzing SSEs and tremor in Mexico, we can clearly distinguish two different sets of behaviors. Slow slip surface displacements in Ja-Co-Mi are very small, while tremor clusters are more isolated and less often activated. In the southwest, tremor in Guerrero and Oaxaca is distributed in a wider belt, active more often, and SSEs are larger. Moreover, tremor duration is longer in Guerrero and Oaxaca (up to 100 s) and shorter in Ja-Co-Mi (around 25 s). We can therefore conclude that slow events in Guerrero and Oaxaca are stronger and similar between each other in those terms. Because we located Oaxaca tremor farther west than previously reported, there is only a 100 km tremor gap between Guerrero and Oaxaca, which could be artificial because of the lack of stations in that zone. Supporting this hypothesis, Zigone et al. (2012) detected triggered LFEs by a beamforming method within this gap (west of station TLIG). This means that there is probably no significant tremor gap between these two provinces. Considering also that SSEs can sometimes propagate to the gap (Graham et al., 2016), add weight to this hypothesis.

Tidal sensitivity analysis shows that tremor in Mexico is sensitive to tides, but the sensitivity is not uniform along the subduction interface. Tremor in Ja-Co-Mi is highly sensitive to tidal shear stress. This is expected since tremor duration is very short (~20 s), and they occur closer to the shore over a dipping plate interface. The tidal sensitivity of tremor in Guerrero and Oaxaca is less clear. The western tremor cluster in Guerrero seems sensitive to tidal shear stress, whereas the eastern cluster does not. On the other hand, the Guerrero eastern cluster, and to a lesser extent Oaxaca tremor, is sensitive to tidal normal stress. This is somewhat surprising, because tidal normal stress is slightly lower than shear stress, and a low coefficient of friction is expected in the tremor source region (e.g., Houston, 2015); thus, it is difficult to explain how normal stress could promote failure considering only tidal loads. Indeed, in this context, with tidal shear stress anticorrelated with tidal normal stress, an increase in tidal normal stress (unclamping) would be related to a decrease in tidal shear stress and would yield a negative variation in the Coulomb failure criterion ($\Delta CFF = \Delta\tau + \mu\Delta\sigma_n$) unless the coefficient of friction is very high. One possibility is that the subduction plane includes local variations in dip; that is, locally, the dip can be −6° instead of +6°. Indeed, close to the coast, the main source

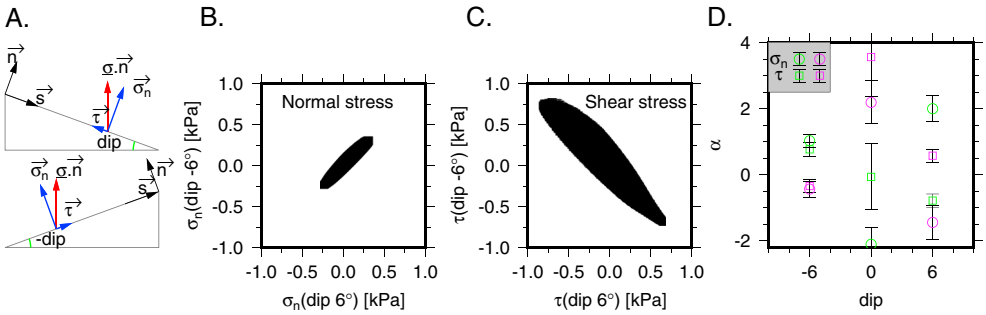

Figure 8. Variation in tidal stress as a function of dip. (a) Cartoon showing the change in tidal shear stress with variation in dip (depending on whether the dip $\vec{\tau}$ is in $\vec{s}$ direction or opposite). (b) Comparison between normal stress calculated for a dip of 6° and −6° for a point in the eastern cluster (green symbols in Figure 8d) during 3 years. The time period of the Guerrero analysis is considered for this comparison. (c) Comparison of shear stress. (d) Tidal sensitivities with respect to tidal shear stress and tidal normal stress. Two points are considered: one in the western cluster (magenta symbols) and one in the eastern cluster (green symbols).

of tidal stress is the ocean tide, whose largest component is radial (σ_{rr}). The tidal shear and normal stresses, induced by σ_{rr} on the fault plane, are

$$\begin{aligned} \tau &= \underline{\sigma}.\vec{n}.\vec{s} = \cos(\text{dip}) \times \sin(\text{dip}) \times \sin(\text{rake}) \times \sigma_{rr} \\ \sigma_n &= \underline{\sigma}.\vec{n}.\vec{n} = \cos^2(\text{dip}) \times \sigma_{rr}. \end{aligned} \tag{7}$$

Thus, if the dip of the subduction plane varies from +6° to −6°, the shear stress induced on the fault plane has the opposite sign, but the normal stress keeps the same sign (Figures 8b and 8c). This is a reasonable hypothesis considering that the moment tensors we obtained sometimes have this characteristic (Figure 7). Moreover, a flat subduction plane is a first-order approximation, and some local variations are likely to exist. This positive correlation, if a variation in dip is present, is consistent with the observations of Peng and Rubin (2017), who reported a tremor recurrence interval close to tidal periodicity in this same patch.

Energy calculations reveal that the energy rate updip in Oaxaca is higher than downdip as was observed in other tremor zones (Yabe & Ide, 2014). The same is not found in Guerrero, presumably because we cannot clearly detect tremors in the updip zone (the transient zone) with this data set. Figure 9 and Table S2 in the supporting information show the relationship between energy rate and moment rate obtained from VLF moment tensor inversion. To estimate the energy rate of stacked events, we use the same normalization process as for identifying VLF velocity waveform (Ide & Yabe, 2014). One stacked energy rate value is the weighted summation of energy (determined between 2 and 8 Hz) divided by tremor duration. The tremor duration is defined as the half-value width of envelopes. We added the values determined by Maury et al. (2016) for VLF events detected by matched filtering. We calculated the energies of events that occurred before the G-GAP experiment using MASE data (Meso America Subduction Experiment, 2007). The values of the energy rate:moment rate ratio are distributed between $3 \cdot 10^{-10}$ and 10^{-9}. This is not surprising, as Ide et al. (2008) demonstrated the proportionality between seismic energy and seismic moment for tremor, VLF, and even longer-period events in Japan, and this proportionality is modeled using a Brownian slow earthquake model (Ide, 2008, 2010a). This model explains various characteristics of slow earthquakes, such as the proportionality between moment and duration (Ide et al., 2007), the flat velocity spectrum across a wide frequency range (Ide et al., 2008), the exponential cumulative density function of the tremor amplitudes (Watanabe et al., 2007), and diffusional migration (Ando et al., 2012; Ide, 2010b). Care must be taken when drawing conclusions, however, because some sources of error are difficult to quantify, especially in the energy rate estimation (see section 7.1). Nevertheless, the similarities among different regions are noteworthy. In a closer look, we can see there is more variability in the Guerrero energy rate values, which is probably caused by using only vertical-component data to estimate the energy, yielding less reliable values. Otherwise, these values are remarkably similar to values obtained in Nankai and Cascadia. This confirms that VLF events and tremor are probably expressions of the same phenomena in different frequency bands around the world. These phenomena seem somewhat different from regular earthquake phenomena, which yields E/M_0 ratios closer to 10^{-5}. These observations suggest that even if there are some variations in the scale of slow events, the underlying processes are similar everywhere.

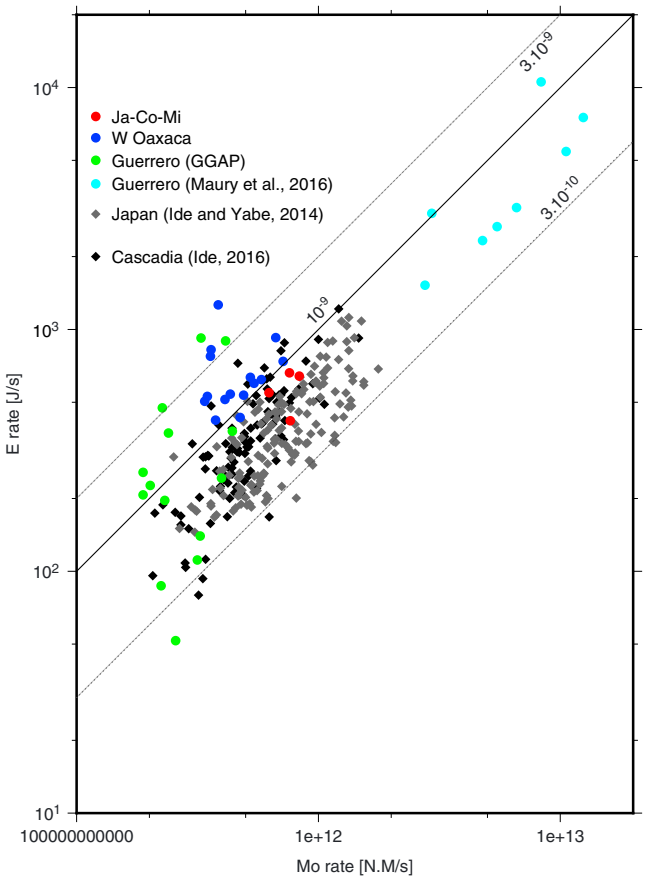

Figure 9. Energy rate as a function of moment rate. Colors correspond to different data sets. Cyan points represent points with moment rates estimated from VLF events detected with a matched filter. Their moment rate com from Maury et al. (2016) and we estimate their energy rate following the method outlined in section 5 (we estimate energy only for events we can locate, that is, 8 events over 11 detected in Maury et al., 2016). All other points are from stacked VLF events, and moment and energy are normalized. The gray lines indicate constant ratio E/Mo. The dotted lines are the bounding values of our observations. The continuous line is the least squares fitting of our observations: $E/Mo = 6 \cdot 10^{-10}$.

Considering the significant differences in slow earthquake behavior along the subduction zone (e.g., near constant activity in some areas, variations in SSE magnitudes and tremor zone width, and the presence of short- and long-term SSEs) the Mexican subduction zone presents variations that are more similar to the Nankai subduction zone than the more homogeneous behavior seen in Cascadia. In addition, large long-term SSEs occur updip from tremors area, while short-term SSEs occur downdip in the sweet spot (Villafuerte & Cruz-Atienza, 2017), similar to that observed in Nankai (Obara & Kato, 2016). However, the tremor area width varies significantly along the Mexican subduction zone interface. The isolated tremor behavior of Ja-Co-Mi led Yabe and Ide (2014) to qualify it as being different from both Cascadia and Nankai, with tremor activity occurring in isolated clusters independent from each other.

7.3. Structural Variations

We observe significant differences between the slow earthquake behavior of the Mexican subduction zone from NW to SE. Here we suggest that variations in the dip of the plate interface are responsible for the variations in slow earthquakes behavior along this subduction zone. This geometrical condition changes the physical properties of the interface, such as the temperature or pressure and so indirectly affects the tremor characteristics that are related to these parameters. The fact that the subduction interface becomes subhorizontal for a distance of ~200 km downdip, at a depth where tremors are often located, may facilitate tremor generation in a wider area. This distinction between the flat subduction plane in Guerrero and the steeper plane in Ja-Co-Mi has already been suggested by Brudzinski et al. (2016) based on differences in the sizes of SSEs.

The temperature on the plate interface is not thought to be directly responsible for slow earthquake generation (Peacock, 2009), but it does affect the mineralogical phase transitions of the interface material accompanied by its dehydration and therefore indirectly influences the zone where slow earthquakes are likely to occur. Den Hartog et al. (2012) suggested that the change from velocity weakening to velocity strengthening depends on temperature. Temperature variations in the New Zealand subduction zone are also consistent with variations in tremor depth (Yabe et al., 2014). The temperature profiles of the Mexican subduction zone show variations from NW to SE (Currie et al., 2002; Ferrari et al., 2012) with higher temperatures in the Rivera-North America plate interface and lower temperatures in the horizontal part of the Cocos Plate. The subducting Cocos Plate in Michoacan is a transition zone between these two provinces. This corresponds well to our observations of tremor variations, with a clear difference between Guerrero-Oaxaca and Ja-Co-Mi; however, some differences are also observed between Michoacan and Jalisco, including variations in energy rate, tidal sensitivity, and tremor depths (Figure 10). Other parameters are also affected by the shape of the subduction plane. Recently, Gao and Wang (2017) suggested that a deep friction zone exists around the mantle wedge corner due to high pore pressure. The ETS would be due to this friction zone. While the cause of the low-velocity zone (Song et al., 2009) over the flat part of the subduction zone in Guerrero is not clear, it has been proposed that this is a mantle relic that was trapped by the flattening of the slab (Manea et al., 2013). The mantle wedge corner would then extend over 100 km, broadening the area where ETS is likely to be present. This would explain the large tremor width observed in this area. Manea et al. (2013) suggested that the variations in slab geometry and fluid release may be the cause of variations in SSEs between Guerrero and Costa Rica; in Costa Rica, the Coco slab plunges steeply and is colder, resulting in a narrow band of low-grade metamorphic dehydration, while in Guerrero the slab dehydration occurs over a wider zone that is consistent with the locations of tremors. The slab in Ja-Co-Mi is warmer than in Costa Rica, but a similar process may cause the observed variations in slow earthquakes. Figure 10 shows our interpretation of interactions between the Mexican subduction zone and slow earthquake characteristics. The slab dips steeply and is warmer in Jalisco, with a mantle wedge corner below

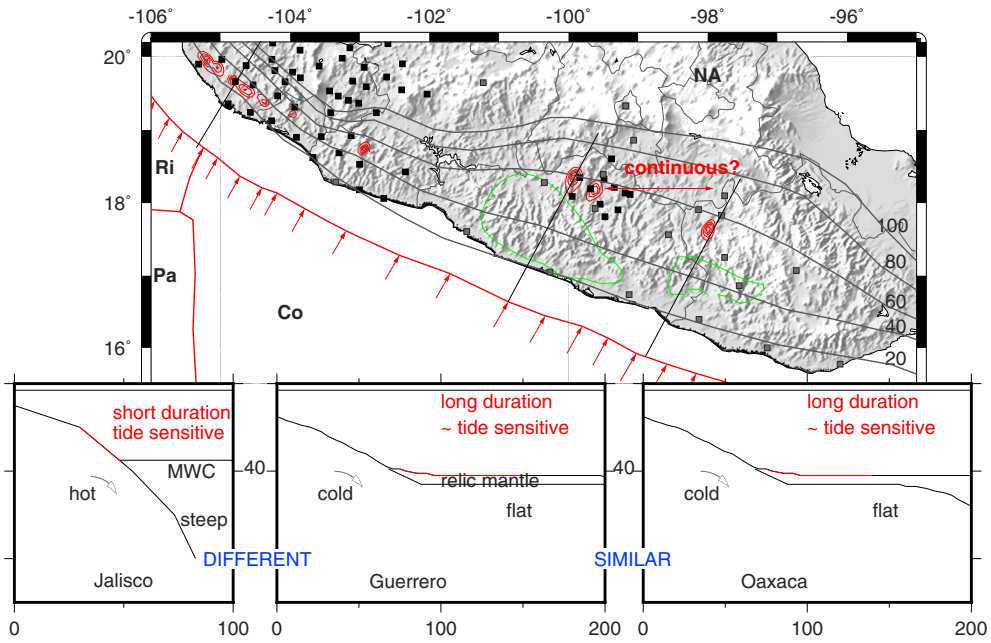

Figure 10. Conceptual illustration summarizing our understanding of the Mexican subduction zone. Red contours indicate tremor density distribution and green contours are typical SSE slip contour for Guerrero and Oaxaca. The cross-section cartoons represent the three different areas considered. The Rivera plate and Northern Coco plates are subducting steeply under the North American plate while the subduction in Guerrero and Oaxaca is flat. As a consequence the slab is warmer under Ja-Co-Mi than under Guerrero and Oaxaca. This impacts the distribution of slow earthquakes (red lines in the cross sections indicate tremor locations) along the subduction in width and duration. MWC: mantle wedge corner.

30 km (Spica et al., 2014), yielding a tremor area of small width with shallow tremors that are strongly sensitive to tide, and very small SSEs. In Guerrero, the slab is flat, colder, and has an extended mantle wedge corner. This produces a wide tremor zone, with tremor being slightly sensitive to tides and larger SSEs. These slow earthquake characteristics extend to western Oaxaca, where the shape of the slab is similar.

Transitions in the behavior of slow earthquakes could correspond to the proposed tears in the subducting plate. Brudzinski et al. (2016) linked a tremor gap beneath the Colima graben to the separation between the Cocos and Rivera plate. Additionally, Stubailo et al. (2012) and Dougherty et al. (2012) proposed that a tear exists in the prolongation of the Orozco Fracture Zone that would separate the Cocos Plate into the North Cocos and South Cocos. The tear would lie between the Michoacan and Guerrero tremor groups.

8. Conclusions

Observations of tremor along the Mexican subduction zone allow us to highlight clear differences between the Ja-Co-Mi region and the Guerrero-Oaxaca region. A change occurs between these two regions in terms of slow earthquake behavior (only short-term SSEs occur, tremor area is narrower, and tremor is very sensitive to tide in Ja-Co-Mi), which is very similar in Guerrero and Oaxaca except for the recurrence intervals of their respective SSEs. Our results also suggest that there is no tremor gap between these two provinces.

Tremors in Ja-Co-Mi are sparse, occurring within a narrow belt and having short durations. They are not very energetic and are highly sensitive to tidal shear stress. In contrast, tremors in Guerrero and Oaxaca are almost continuously active, occurring in large patches with long durations; they are relatively energetic and less sensitive to tidal shear stress. To explain the observed sensitivity to tidal normal stress in Guerrero and Oaxaca, we suggest that local variations in the dip angle of the subduction interface could increase the sensitivity to tidal shear stress.

The tremor energy scaling along the Mexican subduction zone is similar to those observed in other subduction zones, suggesting similarities between events observed in different frequency bands around the world.

Variations in tremor behavior between the northwestern and southeastern segments of the Mexican subduction zone could be due to changes in temperature, which are linked to variations in the dip angle of the plate interface and convergence velocity. The horizontal slab interface in Guerrero and Western Oaxaca creates optimal conditions for tremor generation over a larger area and may explain the unusually wide tremor belt.

Acknowledgments
This research was supported by the Japan/Mexico SATREPS project funded by JST/JICA/UNAM/CONACyT. Comments from anonymous reviewers helped improve this manuscript. We thank Suguru Yabe for providing the code to calculate tidal stress. We thank Xyoli Pérez-Campos for answering any question we had about SSN data. We thank Jose Antonio Santiago, Jorge Real Perez, and the volunteer that made the operation of the G-GAP array possible (G-GAP data are available upon request at IsTerre: https://isterre.fr/recherche/projets-de-recherche/projets-termines/projets-anr/article/projet-g-gap-risque-sismique-associe-a-la-subduction). SSN data were obtained by the Servicio Sismológico Nacional (México), whose staff are acknowledged for station maintenance, data acquisition, and data distribution (http://www.ssn.unam.mx). The G-GAP experiment was funded by the Agence Nationale de la Recherche (France) under contract RA0000CO69 (ANR G-GAP).

References

Agnew, D. (2012). SPOTL: Some programs for ocean-tide loading (SIO Technical Report). Scripps Institution of Oceanography. University of California.

Ando, R., Takeda, N., & Yamashita, T. (2012). Propagation dynamics of seismic and aseismic slip governed by fault heterogeneity and Newtonian rheology. *Journal of Geophysical Research*, *117*, B11308. https://doi.org/10.1029/2012JB009532

Ariyoshi, K., Matsuzawa, T., Ampuero, J.-P., Nakata, R., Hori, T., Kaneda, Y., … Hasegawa, A. (2012). Migration process of very low-frequency events based on a chain reaction model and its application to the detection of preseismic slip for megathrust earthquakes. *Earth Planets Space*, *64*, 693–702. https://doi.org/10.5047/eps.2010.09.003

Brudzinski, M., & Allen, R. (2007). Segmentation in episodic tremor and slip all along Cascadia. *Geology*, *35*, 907–910. https://doi.org/10.1130/G23740A.1

Brudzinski, M., Cabral-Cano, E., Correa-Mora, F., DeMets, C., & Márquez-Azúa, B. (2007). Slow slip transients along the Oaxaca subduction segment from 1993 to 2007. *Geophysical Journal International*, *171*(2), 523–538. https://doi.org/10.1111/j.1365-246X.2007.03542.x

Brudzinski, M., Hinojosa-Prieto, H., Schlanser, K., Cabral-Cano, E., Arciniega-Ceballos, A., Diaz-Molina, O., & DeMets, C. (2010). Nonvolcanic tremor along the Oaxaca segment of the Middle America subduction zone. *Journal of Geophysical Research*, *115*, B00A23. https://doi.org/10.1029/2008JB006061

Brudzinski, M., Schansler, K., Kelly, N., DeMets, C., Grand, S., Márquez-Azúa, B., & Cabral-Cano, E. (2016). Tectonic tremor and slow slip along the northwestern section of the Mexico subduction zone. *Earth and Planetary Science Letters*, *454*, 259–271. https://doi.org/10.1016/j.epsl.2016.08.004

Cruz-Atienza, V., Husker, A., Legrand, D., Caballero, E., & Kostoglodov, V. (2015). Nonvolcanic tremor locations and mechanisms in Guerrero, Mexico, from energy-based and particle motion polarization analysis. *Journal of Geophysical Research: Solid Earth*, *120*, 275–289. https://doi.org/10.1002/2014JB011389

Currie, C., Hyndman, R., Wang, K., & Kostoglodov, V. (2002). Thermal models of the Mexico subduction zone: Implications for the megathrust seismogenic zone. *Journal of Geophysical Research*, *107*(B12), 2370. https://doi.org/10.1029/2001JB000886

DeMets, C., Gordon, R., & Argus, D. (2010). Geologically current plate motions. *Geophysical Journal International*, *181*, 1–80. https://doi.org/10.1111/j.1365-246X.2009.04491.x

den Hartog, S., Peach, C., de Winters, D. M., Piers, C., & Shimamoto, T. (2012). Frictional properties of megathrust fault gouges at low sliding velocities: New data on effects of normal stress and temperature. *Journal of Structural Geology*, *38*, 156–171. https://doi.org/10.1016/j.jsg.2011.12.001

Dougherty, S., Clayton, R., & Helmberger, D. (2012). Seismic structure beneath central Mexico: Implications for the fragmentation of the subducted Cocos Plate. *Journal of Geophysical Research*, *117*, B09316. https://doi.org/10.1029/2012JB009528

Fasola, S., Brudzinski, M., Ghouse, N., Solada, K., Sit, S., Cabral-Cano, E., … Jensen, K. (2016). New perspective on the transition from flat to steeper subduction in Oaxaca, Mexico based on seismicity, nonvolcanic tremor, and slow slip. *Journal of Geophysical Research: Solid Earth*, *121*, 1835–1848. https://doi.org/10.1002/2015JB012709

Franco, S., Kostoglodov, V., Larson, K., Manea, V., Manea, M., & Santiago, J. (2005). Propagation of the 2001–2002 silent earthquake and interplate coupling in the Oaxaca subduction zone, Mexico. *Earth Planets Space*, *57*, 973–985.

Ferrari, L., Orozco-Esquivel, T., Manea, V., & Manea, M. (2012). The dynamic history of the Trans-Mexican volcanic belt and the Mexico subduction zone. *Tectonophysics*, *522–523*, 122–149. https://doi.org/10.1016/j.tecto.2011.09.018

Frank, W., Radiguet, M., Rousset, B., Shapiro, N., Husker, A., Kostoglodov, V., … Campillo, M. (2015). Uncovering the geodetic signature of silent slip through repeating earthquakes. *Geophysical Research Letters*, *42*, 2774–2779. https://doi.org/10.1002/2015GL063685

Frank, W., Shapiro, N., Husker, A., Kostoglodov, V., Romanenko, A., & Campillo, M. (2014). Using systematically characterized low-frequency earthquakes as a fault probe in Guerrero, Mexico. *Journal of Geophysical Research: Solid Earth*, *119*, 7686–7700. https://doi.org/10.1002/2014JB011457

Gao, X., & Wang, K. (2017). Rheological separation of the megathrust seismogenic zone and episodic tremor and slip. *Nature*, *543*(7645), 416–419. https://doi.org/10.1038/nature21389

García, D., Singh, S., Herráiz, M., Ordaz, M., & Pacheco, J. (2005). Inslab earthquakes of Central Mexico: Peak ground-motion parameters and response spectra. *Bulletin of the Seismological Society of America*, *95*, 2272–2282. https://doi.org/10.1785/0120050072

Gomberg, J., & The Cascadia 2007 and Beyond Working Group (2010). Slow slip phenomena in Cascadia from 2007 and beyond: A review. *Geological Society of America Bulletin*, *122*, 963–978. https://doi.org/10.1130/B30287.1

Graham, S., DeMets, C., Cabral-Cano, E., Kostoglodov, V., Rousset, B., Walspersdorf, A., … Salazar-Tlaczani, L. (2016). Slow slip history for the Mexico subduction zone: 2005 through 2011. *Pure and Applied Geophysics*, *121*, 3445–3465. https://doi.org/10.1007/s00024-015-1211-x

Graham, S., DeMets, C., Cabral-Cano, E., Kostoglodov, V., Walpersdorf, A., Cotte, N., … Salazar-Tlaczani, L. (2014). GPS constraints on the 2011–2012 Oaxaca slow slip event that preceded the 2012 March 20 Ometepec earthquake, southern Mexico. *Geophysical Journal International*, *197*(3), 1593–1607. https://doi.org/10.1093/gji/ggu019

Hirose, H., Asano, Y., Obara, K., Kimura, T., Matsuzawa, T., Tanaka, S., & Maeda, T. (2010). Slow earthquakes linked along dip in the Nankai subduction zone. *Science*, *330*(6010), 1502. https://doi.org/10.1126/science.1197102

Houston, H. (2015). Low friction and fault weakening revealed by rising sensitivity of tremor to tidal stress. *Nature Geoscience*, *8*, 409–416. https://doi.org/10.1038/NGEO2419

Husker, A., Kostoglodov, V., Cruz-Atienza, V., & Legrand, D. (2012). Temporal variations of non-volcanic tremor (NVT) locations in the Mexican subduction zone: finding the NVT sweet spot. *Geochemistry, Geophysics, Geosystems*, *13*, Q03011. https://doi.org/10.1029/2011GC003916

Ide, S. (2008). A Brownian walk model for slow earthquakes. *Geophysical Research Letters*, *35*, L17301. https://doi.org/10.1029/2008GL034821

Ide, S. (2010a). Quantifying the time function of nonvolcanic tremor based on a stochastic model. *Journal of Geophysical Research*, *115*, B08313. https://doi.org/10.1029/2009JB000829

Ide, S. (2010b). Striation, duration, migration and tidal response in deep tremors. *Nature*, *466*, 356–359. https://doi.org/10.1038/nature09251

Ide, S. (2016). Characteristics of slow earthquakes in the very low frequency band: Application to the Cascadia subduction zone. *Journal of Geophysical Research: Solid Earth*, *121*, 5942–5952. https://doi.org/10.1002/2016JB013085
Ide, S. (2012). Variety and spatial heterogeneity of tectonic tremor worldwide. *Journal of Geophysical Research*, *117*, B03302. https://doi.org/10.1029/2011JB008840
Ide, S., Beroza, G. C., Shelly, D. R., & Uchide, T. (2007). A scaling law for slow earthquakes. *Nature*, *447*(7140), 76–79. https://doi.org/10.1038/nature05780
Ide, S., Imanishi, K., Yoshida, Y., Beroza, G., & Shelly, D. (2008). Bridging the gap between seismically and geodetically detected slow earthquakes. *Geophysical Research Letters*, *35*, L10305. https://doi.org/10.1029/2008GL034014
Ide, S., & Yabe, S. (2014). Universality of slow earthquakes in the very low frequency band. *Geophysical Research Letters*, *41*, 2786–2793. https://doi.org/10.1002/2014GL059712
Ide, S., Yabe, S., Tai, H.-J., & Chen, K. (2015). Thrust-type focal mechanisms of tectonic tremors in Taiwan: Evidence of subduction. *Geophysical Research Letters*, *42*, 3248–3256. https://doi.org/10.1002/2015GL063794
Idehara, K., Yabe, S., & Ide, S. (2014). Regional and global variations in the temporal clustering of tectonic tremor activity. *Earth Planets Space*, *66*, 66. https://doi.org/10.1186/1880-5981-66-66
Iglesias, A., Singh, S., Lowry, A., Santoyo, M., Kostoglodov, V., Larson, K., & Franco-Sánchez, S. (2004). The silent earthquake of 2002 in the Guerrero seismic gap, Mexico ($M_w = 7.6$): Inversion of slip on the plate interface and some implications. *Geofísica Internacional*, *43*(3), 309–317.
Kao, H., Shan, S.-J., Dragert, H., & Rogers, G. (2009). Northern Cascadia episodic tremor and slip: A decade of tremor observations from 1997 to 2007. *Journal of Geophysical Research*, *114*, B00A12. https://doi.org/10.1029/2008JB006046
Kato, K., Aki, K., & Takemura, M. (1995). Site amplification from coda waves: validation and application to *S*-wave site response. *Bulletin of the Seismological Society of America*, *85*(2), 467–477.
Kostoglodov, V., Husker, A., Shapiro, N., Payero, J., Campillo, M., Cotte, N., & Clayton, R. (2010). The 2006 slow slip event and nonvolcanic tremor in the Mexican subduction zone. *Geophysical Research Letters*, *37*, L24301. https://doi.org/10.1029/2010GL045424
Kostoglodov, V., Singh, S., Santiago, J., Franco, S., Larson, K., Lowry, A., & Bilham, R. (2003). A large silent earthquake in the Guerrero seismic gap, Mexico. *Geophysical Research Letters*, *30*(15), 1807. https://doi.org/10.1029/2003GL017219
Larson, K., Kostoglodov, V., Miyazaki, S., & Santiago, J. (2007). The 2006 aseismic slow slip event in Guerrero, Mexico: New results from GPS. *Geophysical Research Letters*, *34*, L13309. https://doi.org/10.1029/2007GL029912
Lowry, A., Larson, K., Kostoglodov, V., & Bilham, R. (2001). Transient slow slip in Guerrero, southern Mexico. *Geophysical Research Letters*, *28*(19), 3753–3756.
Manea, V., Manea, M., & Ferrari, L. (2013). A geodynamical perspective on the subduction of Cocos and Rivera plates beneath Mexico and Central America. *Tectonophysics*, *609*, 56–81. https://doi.org/10.1016/j.tecto.2012.12.039
Matsuzawa, T., Hirose, H., Shibazaki, B., & Obara, K. (2010). Modeling short- and long-term slow slip events in the seismic cycle of large subduction earthquakes. *Journal of Geophysical Research*, *115*, B12301. https://doi.org/10.1029/2010JB007566
Maury, J., Ide, S., Cruz-Atienza, V., Kostoglodov, V., Gonzáles-Molina, G., & Péres-Campos, X. (2016). Comparative study of tectonic tremor locations: Characterization of slow earthquakes in Guerrero, Mexico. *Journal of Geophysical Research: Solid Earth*, *121*, 5136–5151. https://doi.org/10.1002/2016JB013027
Mazzotti, S., & Adams, J. (2004). Variability of near-term probability for the next great earthquake on the Cascadia subduction zone. *Bulletin of the Seismological Society of America*, *94*(5), 1954–1959.
Meso America Subduction Experiment (2007). Dataset (*Caltech*). https://doi.org/10.7909/C3RN35SP
Nakata, R., Suda, N., & Tsuruoka, H. (2008). Non-volcanic tremor resulting from the combined effect of Earth tides and slow slip events. *Nature Geoscience*, *1*, 676–678. https://doi.org/10.1038/ngeo288
Obara, K. (2011). Characteristics and interactions between non-volcanic tremor and related slow earthquakes in the Nankai subduction zone, southwest Japan. *Journal of Geodynamics*, *52*, 229–248. https://doi.org/10.1016/j.jog.2011.04. 002
Obara, K. (2010). Phenomenology of deep slow earthquake family in southwest Japan: spatiotemporal characteristics and segmentation. *Journal of Geophysical Research*, *115*, B00A25. https://doi.org/10.1029/2008JB006048
Obara, K., & Kato, A. (2016). Connecting slow earthquakes to huge earthquakes. *Science*, *353*, 253–257. https://doi.org/10.1126/science.aaf1512
Pardo, M., & Suárez, G. (1995). Shape of the subducted Rivera and Cocos plates in southern Mexico: Seismic and tectonic implications. *Journal of Geophysical Research*, *100*(B7), 12,357–12,373.
Payero, J., Kostoglodov, V., Shapiro, N., Mikumo, T., Iglesias, A., Péres-Campos, X., & Clayton, R. (2008). Nonvolcanic tremor observed in the Mexican subduction zone. *Geophysical Research Letters*, *35*, L07305. https://doi.org/10.1029/2007JL032877
Peacock, S. (2009). Thermal and metamorphic environment of subduction zone episodic tremor and slip. *Journal of Geophysical Research*, *114*, B00A07. https://doi.org/10.1029/2008JB005978
Peng, Y., & Rubin, A. (2017). Intermittent tremor migrations beneath Guerrero, Mexico, and implications for fault healing within the slow slip zone. *Geophysical Research Letters*, *44*, 760–770. https://doi.org/10.1002/2016GL071614
Radiguet, M., Cotton, F., Vergnolle, M., Campillo, M., Walpersdorf, A., Cotte, N., & Kostoglodov, V. (2012). Slow slip events and strain accumulation in the Guerrero gap, Mexico. *Journal of Geophysical Research*, *117*, B04305. https://doi.org/10.1029/2011JB008801
Radiguet, M., Perfettini, H., Cotte, N., Gualandi, A., Valette, B., Kostoglodov, V., … Campillo, M. (2016). Triggering of the 2014 M_w7.3 Papanoa earthquake by a slow slip event in Guerrero, Mexico. *Nature Geoscience*, *9*(11), 829–833. https://doi.org/10.1038/ngeo2817
Roeloffs, E. (2006). Evidence for aseismic deformation rate changes prior to earthquakes. *Annual Review of Earth and Planetary Sciences*, *34*, 591–627. https://doi.org/10.1146/annurev.earth.34.031405.124947
Shelly, D. (2009). Possible deep fault slip preceding the 2004 Parkfield earthquake, inferred from detailed observations of tectonic tremor. *Geophysical Research Letters*, *36*, L17318. https://doi.org/10.1029/2009GL039589
Song, T.-R. A., Helmberger, D., Brudzinski, M., Clayton, R., Davis, P., Pérez-Campos, X., & Singh, S. (2009). Subducting slab ultra-slow velocity layer coincident with silent earthquakes in southern Mexico. *Science*, *324*(5926), 502–506. https://doi.org/10.1126/science.1167595
Spica, Z., Cruz-Atienza, V., Reyes-Alfaro, G., Legrand, D., & Iglesias, A. (2014). Crustal imaging of western Michoacán and the Jalisco Block, Mexico, from ambient seismic noise. *Journal of Volcanology and Geothermal Research*, *289*, 193–201. https://doi.org/10.1016/j.jvolgeores.2014.11.005
Storchak, D. A., Di Giacomo, D., Bondár, I., Engdahl, E. R., Harris, J., Lee, W. H. K., … Bormann, P. (2013). Public release of the ISC-GEM global instrumental earthquake catalogue (1900–2009). *Seismological Research Letters*, *84*(5), 810–815. https://doi.org/10.1785/0220130034
Stubailo, I., Beghein, C., & Davis, P. (2012). Structure and anisotropy of the Mexico subduction zone based on Rayleigh-wave analysis and implications for the geometry of the Trans-Mexican Volcanic Belt. *Journal of Geophysical Research*, *117*, B05303. https://doi.org/10.1029/2011JB008631

Thomas, A., Nadeau, R., & Bürgmann, R. (2009). Tremor-tide correlations and near-lithostatic pore pressure on the deep San Andreas fault. *Nature*, *462*, 1048–1051. https://doi.org/10.1038/nature08654

Villafuerte, C., & Cruz-Atienza, V. (2017). Insights into the causal relationship between slow slip and tectonic tremors in Guerrero, Mexico. *Journal of Geophysical Research: Solid Earth*, *122*, 6642–6656. https://doi.org/10.1002/2017JB014037

Watanabe, T., Hiramatsu, Y., & Obara, K. (2007). Scaling relationship between the duration and the amplitude of non-volcanic deep low-frequency tremors. *Geophysical Research Letters*, *34*, L07305. https://doi.org/10.1029/2007GL029391

Wech, A. (2010). Interactive tremor monitoring. *Seismological Research Letters*, *81*, 664–669. https://doi.org/10.1785/gssrl.81.4.664

Yabe, S., & Ide, S. (2014). Spatial distribution of seismic energy rate of tectonic tremors in subduction zones. *Journal of Geophysical Research: Solid Earth*, *119*, 8171–8185. https://doi.org/10.1002/2014JB011383

Yabe, S., Ide, S., & Yoshioka, S. (2014). Along-strike variations in temperature and tectonic tremor activity along the Hikurangi subduction zone, New Zealand. *Earth, Planets and Space*, *66*, 142.

Yabe, S., Tanaka, Y., Houston, H., & Ide, S. (2015). Tidal sensitivity of tectonic tremors in Nankai and Cascadia subduction zones. *Journal of Geophysical Research: Solid Earth*, *120*, 7585–7605. https://doi.org/10.1002/2015JB012250

Yang, T., Grand, S., Wilson, D., Guzman-Speziale, M., Gomez-Gonzalez, J., Dominguez-Reyes, T., & Ni, J. (2009). Seismic structure beneath the Rivera subduction zone from finite-frequency seismic tomography. *Journal of Geophysical Research*, *114*, B01302. https://doi.org/10.1029/2008JB005830

Yokota, Y., Ishikawa, T., Watanabe, S., Tachiro, T., & Asada, A. (2016). Seafloor geodetic constraints on interplate coupling of the Nankai trough megathrust zone. *Nature*, *534*, 374–377. https://doi.org/10.1038/nature17632

Zigone, D., Rivet, D., Radiguet, M., Campillo, M., Voisin, C., Cotte, N., … Payero, J. (2012). Triggering of tremor and slow slip event in Guerrero, Mexico, by the 2010 M_w 8.8 Maule, Chile, earthquake. *Journal of Geophysical Research*, *117*, B09304. https://doi.org/10.1029/2012JB009160